

## Microscopic Interdiffusion in Multilayer Structure

Jai-Young Kim

Analytical Engineering Lab., Corporate Technical Consulting & Services Center,  
Samsung Advanced Institute of Technology, P.O. Box 111, Suwon, Korea 440-600

(Received 20 May 1997)

Recently, artificially modulated magnetic multilayer materials, for examples giant magnetoresistant magnetic head materials and magneto-optic recording materials in the wavelength of a blue laser beam, attract great attention in the electronics industry due to their unique properties derived from the modulated multilayer structure. Since the multilayer structure as well as amorphous structure, is non-equilibrium state in terms of free energy, an assessment of the thermal stability in the multilayer structure is crucially important both for basic research and applications. In this review paper, effective microscopic interdiffusion process in the two dimensional multilayer structure will be described in terms of steep concentration gradient effect, strain effect and magnetic transition effect.

### I. Introduction

In the recent advance of magnetic materials science, large numbers of unique and anomalous properties have been obtained by artificially modulated multilayer structure, for examples giant magnetoresistant multilayer materials<sup>(1)</sup> and magneto-optic recording multilayer materials<sup>(2,3)</sup> et al.. Because the artificially modulated multilayer structure is non-equilibrium state in terms of free energy as well as amorphous structure, when it used for devices with thermal energy consumption, the interdiffusion perpendicular to the interface of the multilayer structure progresses so that the changes in structural and physical properties of the multilayer structure are occurred as structure relaxation and crystallization of the amorphous structure do. However, the interdiffusion process as an assessment of thermal stability in the multilayer structure has hardly been surveyed both for theoretically and experimentally.

In this paper, the interdiffusion process in the multilayer structure, which is composed of thin film sublayers is reviewed. Firstly, the comparison between macroscopic and microscopic interdiffusion processes which are applied to three dimensional bulk material and two dimensional multilayer material, respectively will be described from the practical point of view that multilayer structure with a modulation wavelength of less than a few Å in each sublayer is attractive for the device application. In studying the microscopic interdiffusion in the artificially modulated multilayers, extremely low effective interdiffusion

coefficients of the order of  $10^{-27}$  m<sup>2</sup>/sec can be measured using a X-ray diffractometer<sup>(4)</sup>, which is more sensitive than any other methods<sup>(5)(6)(7)</sup>. Then, steep concentration gradient effect, strain effect and magnetic transition effect on the interdiffusion process of the multilayer structure will be characterized by compositional modulation, commensurate-incommensurate transition and paramagnetic-ferromagnetic transition, respectively.

### II. Comparison between macroscopic and microscopic interdiffusion

DuMond and Youtz were the first to artificially produce a compositional modulated Au/Cu multilayer and the first to observe interdiffusion in such a multilayer<sup>(8)</sup>. The X-ray diffraction intensity from the modulated multilayer was found to fall with time indicating that the half-life for the structure is about two days. This suggested a general method for the study of average rates of interdiffusion and the determination of the interdiffusion coefficient of solids in solids by utilizing the decay of the diffraction intensity in such modulated multilayers. This interdiffusion was analyzed by them according to Fick's second law,

$$\frac{dc}{dt} = D \frac{d^2c}{dx^2} \quad (1)$$

c : Atomic fraction of a component in a position x at time t

t : Diffusion time

D : Interdiffusion coefficient in homogeneous system

$x$ : Spatial co-ordinate (normal to the film plane)

They showed that for a sinusoidal composition modulation of wavelength( $\lambda$ ), the intensity( $I$ ) of the corresponding Bragg reflection should decrease according to the following equation,

$$\frac{d[\ln \frac{I}{I_0}]}{dt} = -D \frac{8\pi^2}{\lambda^2} \quad (2)$$

$I_t$  : Intensity of satellite peak after heat treatment during the time  $t$

$I_0$  : Intensity of satellite peak before heat treatment

$D$  : Macroscopic interdiffusion coefficient in non homogeneous system

$\lambda$  : Wave length of compositional modulation

DuMond and Youtz pointed out that higher harmonics in the Fourier series would decay more rapidly so that after some interdiffusion, the compositional modulation would become sinusoidal. To measure a reliable interdiffusion coefficient in the modulated multilayer, the sinusoidal wave form is more suitable than a rectangular one, without any intermetallic compound structure. Only the first order Bragg reflection is observed, and Eq. 2 can be used directly to measure the interdiffusion coefficient.

While the procedure of DuMond and Youtz remains the basis for studies of interdiffusion process in compositional modulated multilayers, they were incorrect in supposing  $D$  in Eq. 2 to be the macroscopic interdiffusion coefficient. In the presence of a steep composition gradient, such as that found in modulated multilayers, Eq. 1 is no longer valid. Since the local free energy in a non-uniform system is dependent not only on the composition at that given point but also on the spatial derivatives of the composition at that point, only the effective microscopic interdiffusion coefficient of the compositional modulated multilayer can be measured using Eq. 2.

Another factor ignored in the DuMond and Youtz analysis is the presence of strain effect in a modulated multilayer which is derived from matrix stress and interfacial stress. The former and the latter in the modulated multilayer can arise from differential thermal contraction or expansion, and different atomic size, respectively. This is especially important when perfect coherence is maintained at the interface of epitaxial multilayers (superlattice multilayers).

In addition to the composition gradient effect and strain effect, Eq. 1 and Eq. 2 may be invalid because  $D$  is composition dependent in a modulated multilayer, and therefore  $D$  in Eq. 2 cannot be the macroscopic interdiffusion coefficient but the effective microscopic one. The consequence is that  $D$  in Eq. 2 is dependent on the wavelength of the multilayer ( $l$ ) and the macroscopic interdiffusion coefficient be obtained only by measuring  $D$

as a function of  $l$ .

Especially in compositional modulated magnetic multilayer, in which only two dimensions need to be considered, the chemical bonding force is weakened due to the loss of symmetry in the crystalline structure, but the magnetic bonding force is significantly enhanced due to the increment of the interfaces per unit volume. Therefore, the magnetic exchange energy as the magnetic bonding force plays an important role in the microscopic interdiffusion process of the magnetic multilayer.

### III. Steep concentration gradient effect on the interdiffusion of multilayer structure

The first analysis of interdiffusion in a steep concentration gradient was given by Hillert<sup>(9)</sup>. He considered a crystalline binary solid solution with compositional variations in one dimension, and showed that the excess local free energy due to a concentration gradient is proportional to the square of that gradient. Hillert considered discrete atomic planes, and found equilibrium composition variations in a system exhibiting spinodal decomposition and ordering, depending on the second differential of Helmholtz free energy.

A different approach for obtaining the free energy of a non-homogeneous system was used by Cahn and Hilliard<sup>(10)</sup>. They considered a continuum in which three dimensional composition variations might arise, and also found that the local free energy depends on the square of the local composition gradient, as pointed out already by Hillert.

The work of Cook et al. combined aspects of both the previous treatments<sup>(11)</sup>. They considered three dimensional compositional variations on a discrete lattice and did not make any assumptions about the thermodynamics of the binary system.

In order to obtain a simple analytic solution of diffusion in a steep concentration gradient, a continuum model is used firstly, restricted to compositional variation in one dimension perpendicular to multilayer plane which is reasonable for a compositional modulated multilayer. A discrete model is modified later to compare with the continuum model for short wavelength multilayers. In a homogeneous system, the local free energy depends on the composition at a given point, but in a non-homogeneous system, the local free energy depends not only on the local composition but also on the composition of the surrounding volume. The total free energy in a non-homogeneous system is expressed as follows,

$$F = A \int [f_0(c) + K(\frac{dc}{dx})^2] dx \quad (3)$$

$F$  : Total free energy in non-homogeneous system

$A$  : Cross-sectional area of the system normal to the  $x$  axis

$f_0$  : Helmholtz free energy per unit volume of the homogeneous solution

K : Gradient energy coefficient

According to the theories for a compositional non-homogeneous system, mentioned above, a correction should be applied to Fick's law of Eq. 1 for chemical diffusion if the interdiffusion distances are small. This correction comes from the effect of steep composition gradients on the thermodynamic driving force. From the theory, the following linearized diffusion equation is given by

$$\frac{dc}{dt} = D \frac{d^2c}{dx^2} - \frac{2D}{\Gamma''} K \frac{d^2c}{dx^2} \quad (4)$$

c : Atomic fraction of a component in a position x at time t

D : Interdiffusion coefficient ( composition modulation is infinite)

$\Gamma''$  : Second derivative of the Helmholtz free energy of a homogeneous phase per unit volume

The second term of Eq. 4 cannot be neglected when the variation of composition with distance contains a Fourier component with wavelength less than about 100 Å. For composition modulations of small amplitude, it is reasonable to assume that D,  $\Gamma''$  and K are independent of the composition. Under these conditions, a particular solution is

$$c - c_0 = \exp \left[ -D \beta^2 \left( 1 + \frac{2K\beta^2}{\Gamma''} \right) t \right] \cos \beta x \quad (5)$$

$$= A \cos \beta x$$

$c_0$  : Composition of the homogeneous system

$\beta$  : Wave number of the composition wave ( $2\pi/\lambda$ )

A : Amplitude of the composition wave  $\{ = \exp(-D_{eff}\beta^2)t \}$

This cosine wave in composition may decay or grow in amplitude(A), depending on the sign of the amplification factor(R):

$$\frac{d(\ln A)}{dt} = R = -D \left( 1 + \frac{2K\beta^2}{\Gamma''} \right) \beta^2 = -D_{eff}\beta^2 \quad (6)$$

R : Amplification factor ( $= -D_{eff}\beta^2$ )

$D_{eff}$  : effective interdiffusion coefficient

The effective microscopic interdiffusion is dependent on the wavelength of the composition modulation. If there is no gradient effect, the interdiffusion coefficient would be independent of the wavelength. It should be noted that in the analysis of DuMond and Youtz Eq. 2 is correct if the effective interdiffusion coefficient ( $D_{eff}$ ) is substituted for the macroscopic interdiffusion coefficient (D).  $D_{eff}$  is given as follows, and D can be calculated,

$$D_{eff} = D \left( 1 + \frac{2K\beta^2}{\Gamma''} \right) \quad (7)$$

the quantities,  $\Gamma''$  and K, can be evaluated for a regular solution model<sup>(10)</sup>;

$$\Gamma'' = 4[ RT - 2 H_m ] / V \quad (8)$$

$$K = 2 H_m r^2 / 3V \quad (9)$$

$H_m$  : Energy of mixing per mole of equiatomic solution

V : Molar volume

r : Nearest neighbour distance

The macroscopic interdiffusion coefficient (D) is replaced by the effective interdiffusion coefficient ( $D_{eff}$ ), which can be determined using Eq. 2 from the slope of the best straight line fit through the linear portion in the  $\ln(I_t/I_0)$  of the first satellite peak versus heat-treated time (t) plot.

The continuum model has the advantage of simplicity, but breaks down at low wavelength, especially in the perfect coherent state. This problem can be solved only by taking a fully microscopic approach, such as the discrete model in the work of Cook et al.<sup>(11)</sup>. They derived the analogue of Eq. 3 for atomic interchange between discrete sites and considered diffusion in a general direction in simple cubic, bcc and fcc structures. In the special cases of diffusion along the  $\langle 100 \rangle$  or  $\langle 110 \rangle$  directions in the bcc structure, or along  $\langle 100 \rangle$  or  $\langle 111 \rangle$  in the fcc structures, their treatment is simplified, and the amplification factor (R) for a harmonic wave is given by an expression of the form of Eq. 6, in which the wave number squared  $\beta^2$  is replaced by the function  $\beta^2$ , given by the dispersion relation

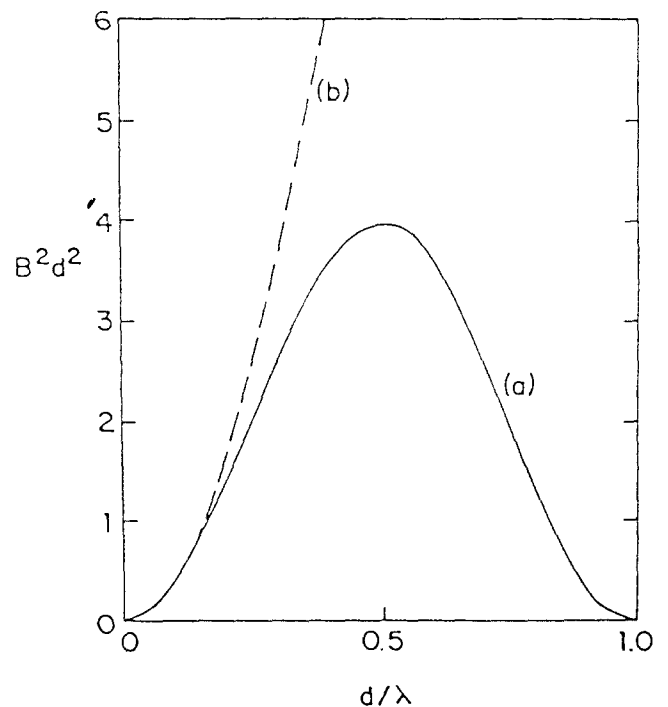


Fig. 1: A comparison of the discrete and continuum models of multilayer structure [H. E. Cook and D. de Fontaine, Acta Metall 17 (1969) 915]

$$B^2 = (2/d^2)[1 - \cos(2\pi d/\lambda)] \quad (10)$$

where  $d$  is the spacing between the atomic planes perpendicular to the diffusion direction in the multilayer. Note that for  $\lambda \gg d$ , the cosine can be expanded and  $\beta^2 = 4\pi^2/\lambda^2$ , the value of  $\beta^2$  in the continuum model. The two models are compared in Fig. 1.<sup>(11)</sup> In the discrete model, the behaviour is symmetric about  $\lambda = 2d$ . It can be seen that the continuum model is a good approximation for  $\lambda > 6d$ . For single crystalline materials, an analysis based on that of Cook et al. is most appropriate; for amorphous and polycrystalline materials the continuum analysis is adequate<sup>(11)</sup>.

#### IV. Strain effect on the interdiffusion of multilayer structure

The first treatment of the strain effect on the free energy of a compositional modulated solid was done by Cahn<sup>(12)</sup>. He considered a three-dimensional isotropic solid with no long-range elastic strain fields. In a crystal of this type, with no structural imperfection, coherency strain will arise if the molar volume is a function of composition. Provided that the amplitude of compositional modulation is sinusoidal, it is reasonable to suppose that no dislocation will arise as a consequence of the modulation. The total free energy of the system ( $F$ ) is given by

$$F = A \int [f_0(c) + K \left(\frac{dc}{dx}\right)^2 + \frac{n^2 E}{1-\nu} (c - c_0)^2] \quad (11)$$

$E$ : Young's modulus for average composition  $c_0$

When strain effects are present, the expression for the amplification factor becomes

$$R = -D[1 + (2K\beta^2/f_0'') + (2n^2 E/f_0''(1-\nu))\beta^2] \beta^2 = -D_{eff}\beta^2 \quad (12)$$

When the anisotropy in the elastic strain energy is applied, the amplification factor for a harmonic wave is given by,

$$R = -D[1 + (2K\beta^2/f_0'') + (2n^2/f_0'')Y(UVW)] \beta^2 \quad (13)$$

$Y(UVW)$ : a modulus, depending on the direction  $[UVW]$  of the wave vector of the composition modulation.

For the high-symmetry direction  $\langle 100 \rangle$ ,  $\langle 110 \rangle$ , and  $\langle 111 \rangle$  in a cubic crystal,  $Y(UVW)$  is given by

$$Y(UVW) = \frac{1}{2}(C_{11} + 2C_{12}) \times \left[ 3 - \frac{C_{11} + 2C_{12}}{C_{11} + 2(2C_{44} - C_{11} + C_{12})(l^2 m^2 + m^2 n^2 + n^2 l^2)} \right] \quad (14)$$

$C_{11}$ , etc.: Stiffness coefficient

$l, m, n$ : Direction cosine of the direction  $\langle UVW \rangle$  with respect to the cubic axes.

The continuum model used by itself is no longer valid when the elastic strains vary over distances similar to inter-atomic spacing in the crystal. In this case, discrete analysis must be used(11)(13). In general conclusion for the discrete model, the contribution of elastic strain energy to the bulk free energy of a solid solution is significant, at least when the atomic size difference exceeds 4 %. In contrast to the results for the continuum model, it was found that the excess free energy of a system due to a harmonic composition modulation depends not only on the direction, but also on the magnitude of the modulation wavelength in a commensurate-incommensurate (CI) transition. This wavelength dependence can be described by using an effective modulation( $M(UVW)$ ) to replace  $Y(UVW)$  for high symmetry directions in cubic crystals, and the ( $M(UVW)$ ) is dependent only on  $d/\lambda$ , where  $l$  is the modulation wavelength and  $\lambda$  is the spacing between the atomic planes perpendicular to  $(UVW)$ .

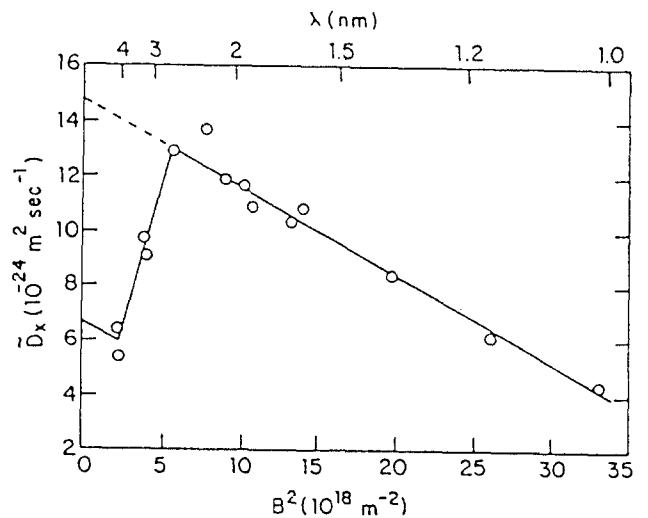


Fig. 2: Variation of the effective microscopic interdiffusion coefficients ( $D_{eff}$ ) in Cu/Pd modulated multilayers with  $B^2$  for discrete model and  $\lambda$  for continuum model heat-treated at 389°C [E. M. Philofsky and J. E. Hilliard, J. Appl. Phys. 40 (1969) 2198]

Fig. 2 shows the variation of effective microscopic interdiffusion coefficient ( $D_{eff}$ ) in Cu/Pd modulated multilayers (82 at. % Pd) with  $B^2$  for discrete model and  $\lambda$  for continuum model at 389°C<sup>(14)</sup>. On the figure, the plot is linear for  $\lambda < 2.8$  nm, but at larger wavelength  $D_{eff}$  is approximately halved. Such a drop in the  $D_{eff}$  suggests a loss of coherency in the multilayers since, if the layers are incoherent, the coherent strain energy contribution to  $D_{eff}$  is lost. In the continuum treatment of strain effects in coherent modulated multilayers, it is found that the elastic energy due

to the modulation is independent of its wavelength. On the other hand, if the difference in lattice parameter between the sublayers in a multilayer is accommodated by misfit dislocations, the excess strain energy due to the dislocations will be proportional to the number of interfaces and therefore inversely proportional to the wavelength. The coherent strain energy per unit volume is constant, whereas the misfit dislocation energy varies as the number of interfaces per unit volume in the multilayer. It is expected, that as the wavelength is increased, at a critical point which is  $d/6\lambda^{(11)}$  ( $d$ : lattice parameter in multilayer,  $\lambda$ : wavelength in multilayer), the dislocation energy will become energetically favourable for the sublayers in a modulated multilayer to be partially coherent or incoherent. Using low-angle grain boundary data for Cu, Philofsky estimated from a simple energy balance that coherency should be lost for wavelength greater than 2.5 nm<sup>(14)</sup>. The experimental values of the ratio are plotted in Fig. 3, together with calculated values for incoherent and coherent modulation<sup>(15)</sup>. It is clear from Fig. 3 that the modulation is coherent for  $\lambda < 2.8$  nm and incoherent for  $\lambda > 3.8$  nm. It is interesting to note that there is gradual loss of coherency. The partial coherency at intermediate  $\lambda$  may be an equilibrium state since the corresponding values of  $D_{eff}$  appears to remain constant in the terminal stages of heat treatment.

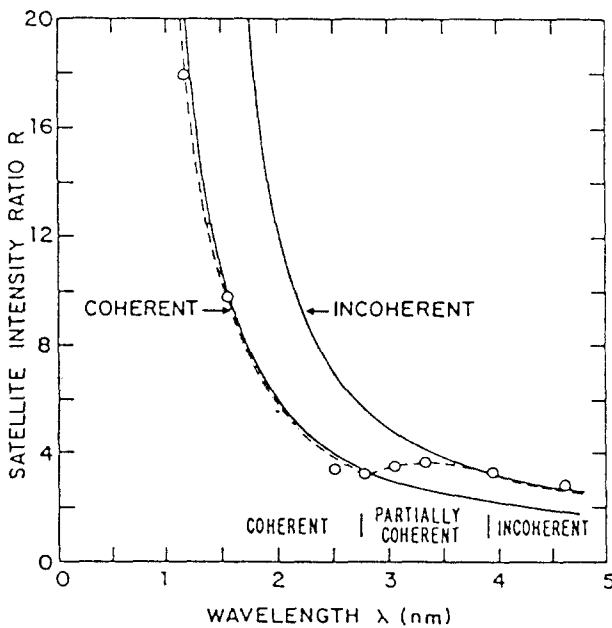


Fig. 3: Plots of the ratio R of the intensity of the 111-satellite to that of the 111+ satellite as a function of modulated wavelength in Cu/Pd multilayers (80 at. % Pd) [E. M. Philofsky and J. E. Hilliard, J. Appl. Phys. 40 (1969) 2198]

In the X-ray measurement for the effective interdiffusion coefficient, when the diffusion process is linear, the slope of the  $\ln \frac{I_t}{I_0}$  is

$$\frac{d[\ln \frac{I_t}{I_0}]}{dt} = -D_{eff} \frac{8\pi^2}{\lambda^2} \quad (15)$$

- $I_0$  : X-ray intensity of satellite peak before heat treatment
- $I_t$  : X-ray intensity of satellite peak after heat treatment for (t) seconds
- $D_{eff}$  : Effective interdiffusion coefficient
- $\lambda$  : Wavelength of the x-ray
- $m$  : Order of diffracted satellite peak in small angle

from which the effective interdiffusion coefficients in the continuum model can be determined directly. In the discrete approach, this becomes

$$\frac{d[\ln \frac{I_t}{I_0}]}{dt} = \frac{4D_{eff}}{d^2} [1 - \cos(2\pi md/\lambda)] \quad (16)$$

- $d$  : Spacing between the atomic planes perpendicular to the diffusion direction.

Since the composition gradient in the continuum model and both the composition gradient and strain effects in the discrete model are included in both of the above equations, effective interdiffusion coefficients ( $D_{eff}$ ) are determined from the slope of the best straight line fit through the linear portion of the  $(\ln \frac{I_t}{I_0})$  vs. heat-treated time (t) plot of the first satellite peak.

### V. Magnetic transition effect on the interdiffusion of multilayer structure

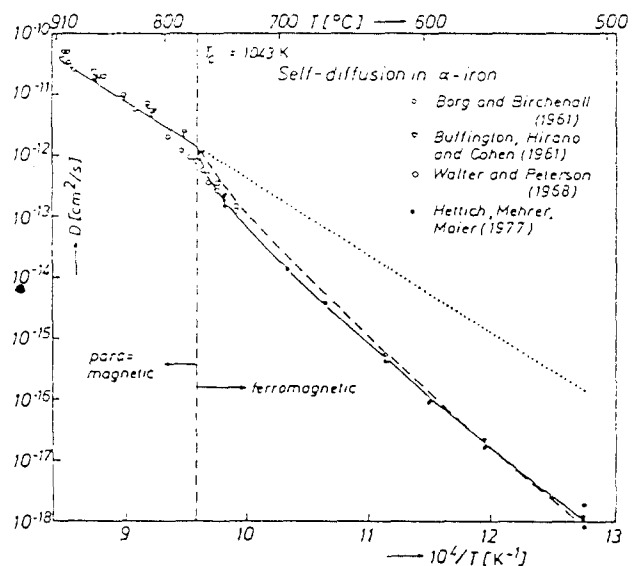


Fig. 4: Arrhenius plot of self-diffusion in paramagnetic and ferromagnetic  $\alpha$ -iron [G. Hettich, H. Mehrer and K. Maier, Scripta Metallurgica 11 (1977) 795]

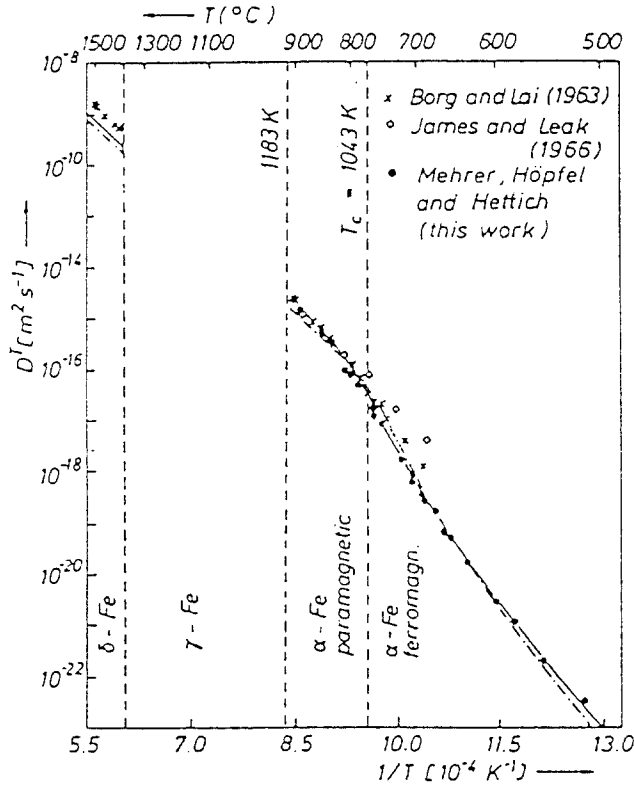


Fig. 5: Arrhenius diagram for the impurity diffusion of Co in bcc  $\alpha$ - and  $\gamma$ -iron [H. Mehrer, D. Höpfel and G. Hettich, *Dimeta-82* (1983) 360]

Diffusion experiments of magnetic transition effect were conducted in self-diffusion and interdiffusion in bulk materials by means of a radio-tracer method in combination with a conventional mechanical sectioning and sputter-sectioning methods. Fig. 4 and Fig. 5 display Arrhenius plots of self-diffusion in  $\alpha$ -Fe<sup>(16)</sup> and interdiffusion of Co in  $\alpha$ -Fe<sup>(17)</sup>, respectively. In both of the diffusion processes, the temperature dependence of their diffusion coefficients show a strong deviation from the Arrhenius type behaviour due to the influence of the transition from ferromagnetic to paramagnetic at Curie temperature. The diffusion coefficients in the magnetically ordered ferromagnetic state are considerably lower than those estimated by extrapolation of the data from the disordered paramagnetic state<sup>(18)(19)(20)(21)(22)</sup>.

From general consideration, at sufficiently low temperatures bulk self-diffusion in metals is dominated by mono-vacancies. The diffusion coefficient as measured by the radio-tracer method may be written as

$$D = f a^2 m \exp \left[ - \left( \frac{G^F + G^M}{kT} \right) \right] \quad (17)$$

$f$  : Correlation factor

$a$  : Lattice parameter

$m$  : Attempt frequency for vacancy migration.

$$G^F = H^F - TS^F \text{ and } G^M = H^M - TS^M \quad (18)$$

(Gibb's free energies of vacancy formation (F) and motion (M))

Whereas usually the enthalpies ( $H^F$ ,  $H^M$ ) and entropies ( $S^F$ ,  $S^M$ ) are almost independent of temperature, in a ferromagnetic metal a temperature variation of these quantities may be expected due to the influence of the magnetic spin order. The Arrhenius plot of diffusion coefficient ( $D$ ) can then no longer be approximated by a straight line but shows strong curvature. From Eq. 17 and  $\frac{d(G/T)}{d(1/T)} = H$ , it follows that the slope of the curved Arrhenius plot is given by

$$- \frac{d \ln D}{d(1/kT)} = Q \quad (19)$$

where  $Q = H^F + H^M$  denotes the (temperature dependent) activation energy of diffusion. The temperature variation of the enthalpies and entropies are coupled through the thermodynamic relationship

$$\left( \frac{dH^F + M}{dT} \right)_P = \left( \frac{dS^F + M}{dT} \right)_P \quad (20)$$

which leads to a temperature dependence of the pre-exponential factor

$$D^0 = f a^2 m \exp \left( \frac{S^F + S^M}{k} \right) \quad (21)$$

when Eq. 17 is written in the usual form

$$D = D^0 \exp \left( \frac{-Q}{kT} \right) \quad (22)$$

A temperature dependence of the activation parameters below the Curie temperature is obvious from Fig. 4 and Fig. 5

A theoretical treatment of the influence of ferromagnetic ordering on diffusion has been given by Lee Ruch et al.<sup>(23)</sup> in analogy to similar effects in order-disorder alloys. Their result may be written as

$$G^{F,M} = G^{F,M} + \Delta G^{F,M} \quad (23)$$

and

$$\Delta G^{F,M} = \alpha^{F,M} R^2 \quad (24)$$

$$R = \frac{M_S(T)}{M_S(0)} \quad (25)$$

denotes the ferromagnetic order parameter.  $M_S(T)$  is the spontaneous magnetization of the ferromagnetic state at temperature ( $T$ ). The subscript (P) refers to the paramagnetic state, for which the enthalpies ( $H_P^F$ ,  $H_P^M$ ) and entropies ( $S_P^F$ ,  $S_P^M$ ) are assumed to be independent of temperature. The parameter

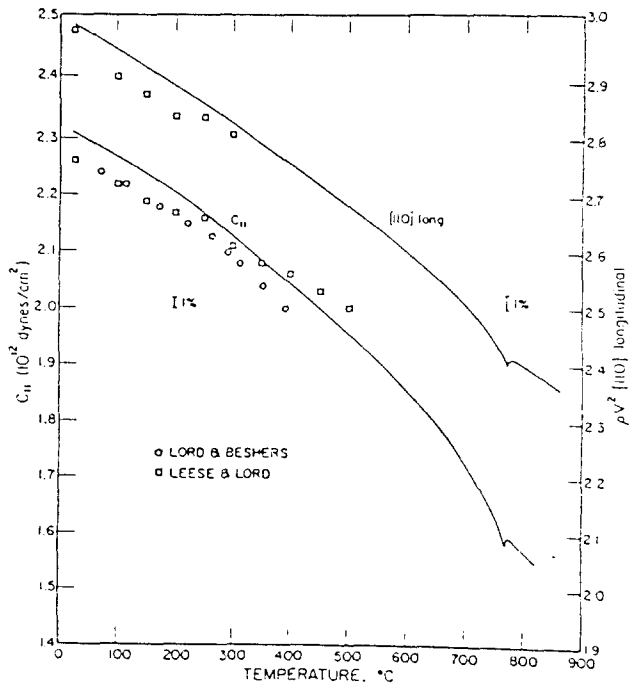


Fig. 6: Temperature dependence of measured longitudinal elastic constant of  $\alpha$ -iron [D. J. Dever, J. Appl. Phys. 43 (1972) 3293]

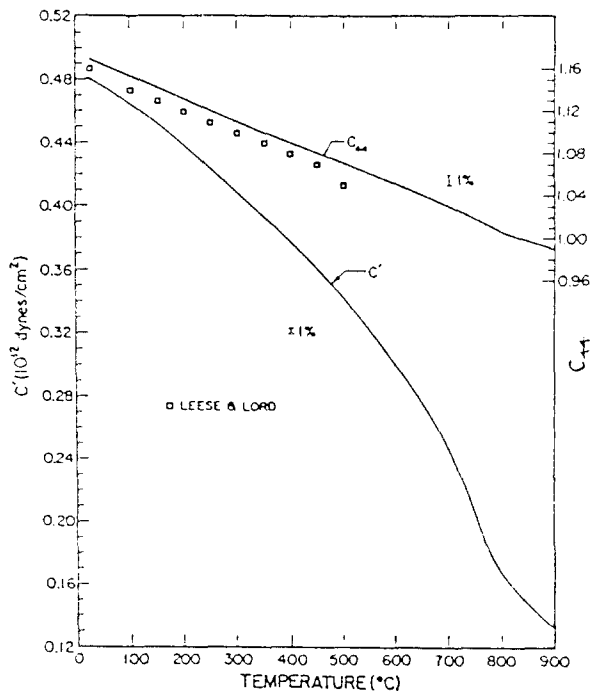


Fig. 7: Temperature dependence of measured shear elastic constant of  $\alpha$ -iron [D. J. Dever, J. Appl. Phys. 43 (1972) 3293]

$$\alpha^l = 0.5 ZJ \tag{26}$$

is related to the exchange integral (J) and the co-ordination number (Z). The  $\alpha^l$  is found to be 0.045 eV/atom in a-

iron(16). The parameter  $\alpha^M$  has to be determined from a comparison with experiment. Substituting Eq. 23, 24, 25 and 26 into Eq. 17 gives

$$D = D_p^0 \exp \{-Q_p(1 + \alpha R^2)/kT\} \tag{27}$$

$$D_p^0 = f a^2 m \exp \left\{ \frac{(S_p^l + S_p^M)}{k} \right\}$$

$$Q_p = H_p^l + H_p^M$$

$$\alpha = \frac{(\alpha F + \alpha M)}{Q_p}$$

$D_p^0$  and  $Q_p$  denote the pre exponential factor and the activation energy in the paramagnetic state and are taken as temperature independent. Eq. 27 explains the non linearity in the Arrhenius plot below  $T_c$  to the temperature dependence of the ferromagnetic order parameter (R). At low temperatures R approaches unity and Eq. 27 then becomes a simple Arrhenius law again. The activation energy for the fully ordered ferromagnetic state is  $Q_f = Q_p(1+\alpha)$  whereas the pre-exponential factor is the same as in the paramagnetic state. Difference in the activation energy between ferromagnetic and paramagnetic states is proportional to the product of exchange integral and co-ordination number which represents magnetic exchange energy.

Research into the influence of ferromagnetic ordering on diffusion was conducted by D. J. Dever<sup>24</sup>. In this research, a remarkable non-linear temperature dependence of elastic constants associated with ferromagnetic ordering was observed in single crystal Fe. On Fig. 6 and Fig. 7, a large difference in magnetic effect exists between the two shear constants  $C'$  and  $C_{44}$ <sup>24</sup>. The normal temperature dependence of the elastic constants above the Debye temperature should be linear<sup>25</sup>. In addition, the temperature dependence of the shear constants should be much less than that of the

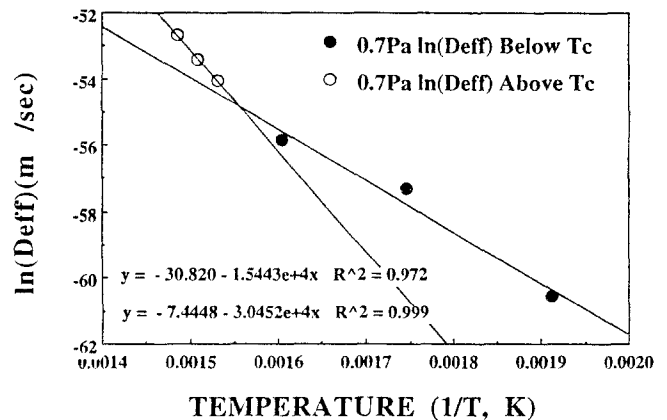


Fig. 8: Arrhenius plots of effective interdiffusion coefficients (Deff) in the Co/Pd multilayers as a function of reciprocal heat treatment temperature [Jai-Young Kim, Sc. Ph. D. Dissertation, Cambridge university, Cambridge, UK (1994)]

longitudinal constants, primarily because of the smaller volume dependence of the shear module. However, as can be seen in Fig. 6 and Fig. 7,  $\alpha$ -Fe is an exception, inasmuch as the anomalous temperature dependence reaches a peak at the Curie temperature. An obvious explanation of such an anomaly could be the magnetic property of Fe. A similarity of temperature dependence may be seen between the magnetic properties and the elastic constants<sup>(26)</sup>. This implies that elastic moduli are dependent on the amount of spin order related each other. In magnetic materials, magnetic spins try to expand their distance to reduce magnetostatic energy, as far as elastic strain energy is allowed at their lattice points. As a result, the total energy is the minimum sum of the two<sup>(27)</sup> in the magnetic materials. Because of the above relationship between magnetic order energy and elastic strain energy, a remarkable non-linear temperature dependence of elastic constants associated with ferromagnetic ordering occurs.

Effective microscopic interdiffusion experiment of magnetic transition effect on the artificially modulated Co/Pd magnetic multilayer was conducted by Jai-Young Kim as shown on Fig. 8<sup>(28)</sup> which displays Arrhenius plot of effective interdiffusion coefficients in Co/Pd multilayers with respect to the reciprocal heat treatment temperature ( $1/T$ ). On the Fig. 8, 3 points in the paramagnetic region lie on linear slope, but the other 3 points in the ferromagnetic region lie on another linear line. Activation energy of the Co/Pd multilayers in ferromagnetic and paramagnetic states is 253 kJ/mole and 128 kJ/mole, respectively which is calculated by slope of Arrhenius equation.

Comparing with previous researches in  $D_{eff}$  which found activation energies of 115 kJ/mole in Mo/Ge<sup>(29)</sup>, 105 kJ/mole in Mo/Si<sup>(29)</sup>, 103 kJ/mole in Pb/Mg<sup>(30)</sup>, 141 kJ/mole in Cu/Au<sup>(31)</sup> and 106 kJ/mole in Cu/Ni<sup>(32)</sup> non-multilayers, the activation energy of the Co/Pd multilayers in the paramagnetic state is comparable to these values. However, the activation energy in the ferromagnetic state is almost as twice as that in the paramagnetic state.

### Summary

The effective microscopic interdiffusion process in the artificially modulated multilayer structure was reviewed in terms of steep concentration gradient effect, strain effect and magnetic transition effect. Compared with the macroscopic interdiffusion in the three dimensional bulk structure, the microscopic interdiffusion in the two dimensional multilayer structure is strongly affected by heterogeneous compositional gradient, incoherent-coherent strain transition and paramagnetism-ferromagnetism transition. In the fabrication and utilization of multilayer devices, these factors should be considered in the multilayer structure as an assessment of thermal stability.

### References

1. S. S. P. Parkin, R. Bhadra and K. P. Roche, Phys. Rev. Lett, **66**, 2152 (1991).
2. F. J. A. denBroeder, H. C. Donkersloot, H. J. G. Draaisma and W. J. M. de Jonge, J. Appl. Phys, **61**, 4317 (1985).
3. S. Hashimoto, Y. Ochiai and K. Aso, J. Appl. Phys, **66**, 4909 (1989).
4. A. L. Greer and F. Spaepen, Chapter 11, *Synthetic Modulated Structure* Ed. by L. L. Chang and B. G. Giessen, Academic press, 561 (1985).
5. F. E. Luborsky and F. Bacon, Proc. Int. Conf. Rapidly Quenched Metal 4th (T. Masumoto and K. Suzuki, Eds), 561 (1982).
6. R. W. Cahn, J. E. Evetts, J. Patterson, R. E. Somekh and C. Kenway-Jackson, J. Mater. Sci, **15**, 702 (1980).
7. D. Gupta, K. N. Tu and K. W. Asai, Phys. Rev. Lett, **35**, 796 (1975).
8. J. DuMond and J. P. Youtz, J. Appl. Phys, **34**, 2633 (1936).
9. M. Hillert, Sc. Ph. D. thesis, Massachusetts Institute of Technology, Cambridge, Massachusetts (1956).
10. J. W. Cahn and J. E. Hilliard, J. chem. and phys, **28**, 28 (1958).
11. H. E. Cook and D. de Fontaine, Acta Metall, **17**, 915 (1969).
12. J. W. Cahn, Acta. Metall, **9**, 795 (1961).
13. H. E. Cook and D. de Fontaine, Acta Metall, **19**, 607 (1971).
14. E. M. Philofsky and J. E. Hilliard, J. Appl. Phys, **40**, 2198 (1969).
15. E. M. Philofsky, Ph. D thesis, Northwestern University, Evanston, Illinois (1968).
16. G. Hettich, H. Mehrer and K. Maier, Scripta Metallurgica, **11**, 795 (1977).
17. H. Mehrer, D. Hopfel and G. Hettich, Dimeta-82 360 (1983).
18. R. J. Borg and C. E. Birchenall, Trans. Met. Soc. AIEM, **218**, 980 (1961).
19. F. S. Buffington, K. Hirano and M. Cohen, Acta Met, **9**, 434 (1961).
20. C. M. Walter and N. L. Peterson, Phys. Rev, **178**, 922 (1968).
21. R. J. Borg and D. Y. F. Lai, Acta. Met, **11**, 861 (1963).
22. D. W. James and G. M. Leak, Phil. Mag, **12**, 701 (1966).
23. L. Ruch, D. R. Sain, H. L. Yeh and L. A. Girifalco, J. Phys. Chem. Sol, **37**, 649 (1976).
24. D. J. Dever, J. Appl. Phys, **43**, 3293 (1972).
25. H. B. Huntington, *Solid State Physics*, Ed. by F. Seitz and D. Turnbull Vol. 7 (Academic, New York) 328 (1958), .



26. E. S. Fisher, C. N. Reid, J. L. Routhort and D. J. Dever, *Acta Met*, **19**, 1307 (1971).
27. S. Chikazumi, *Physics of Magnetism* (John Wiley & Sons, New York, 161 (1964).
28. Jai-Young Kim, Sc. Ph. D. Dissertation, Cambridge university, Cambridge, UK (1994).
29. E. M. Philofsky and J. E. Hilliard, *J. Appl. Phys.*, **40**, 2198 (1969).
30. W. B. Pearson, *Crystal chemistry and physics of metals and alloys*, Wiley (1972).
31. J. Dinklage and R. Frerichs, *J. Appl. Phys.*, **34**, 2633 (1963).
32. W. M. Paulson and J. E. Hilliard, *J. Appl. Phys.*, **48**, 2117 (1977).